Estimation of backscattered echoes from underwater targets using block sparsity

Xiangxia Meng, Xiukun Li
Acoustic Science and Technology Laboratory,
Harbin Engineering University
College of Underwater Acoustic Engineering,
Harbin Engineering University
Harbin 150001, China
{mengxiangxia, lixiukun}@hrbeu.edu.cn

Andreas Jakobsson
Department of Mathematical Statistics,
Lund University
SE-221 00 Lund, Sweden
aj@maths.lth.se

***Abstract*—In this work, we introduce a block sparse reconstruction technique to estimate backscattered echoes from underwater targets. The backscattered field of a spherical shell or the broadside scattering of a cylindrical shell contains a specular reflection as well as some elastic leaky surface waves, while the elastic parts appear as a periodic signal, which may be modeled using a block pattern. Thus, the parameters detailing the reflectors may be estimated using a convex optimization problem imposing the expected block structure. Numerical simulations and experiment results indicate the performance of the proposed method.**

I. Introduction

Underwater target detection and classification is a challenging but important problem, being of interest in a wide range of applications. Low-frequency sonar systems are often used for such problems, especially when one wishes to identify objects that are partly or fully submerged in the bottom sediments, as such systems may offer a large detection range and suffer low propagation loss when penetrating into the sediments. Moreover, it has been demonstrated that in the frequency range where the wavelength is comparable with the target dimension, the acoustic scattering features involving the elastic response can be measured [1], which may in turn provide relevant information for target identification. In order to develop a robust and effective procedure exploiting the scattered acoustic response, it is necessary to model the relationship between the characteristics of the scattering echoes and the physical structure and behavior of the studied objects. As may be expected, several earlier studies have investigated this relationship, examining comparisons in the time domain [2], the frequency domain [3], [4], as well as in the aspect angle domain [5], for varying environments and scattering geometries. Some studies examining the signal's time-frequency distributions have also been made [6], [7].

In this paper, we build on these works and consider the problem of estimating and enhancing the elastic parts of the backscattered echoes. Herein, we exploit that the backscattered response from a spherical or a cylindrical shell may be well modeled as a sequence of echo pulses, consisting of specular reflections and elastic waves. The latter parts mainly result from the reradiation of leaky surface waves [8]. Due to the attenuation effects, these waves might be much weaker than the specular parts, making them hard to detect and analyze. To solve this problem, some noteworthy topics have investigated such as high-resolution estimators [9], the rigid and elastic separation method [10], as well as array processing techniques [11]. Generally, these methods consider each of the signal components separately, ignoring the detailed structure of the overall sequence. For a spherical shell, quantitative ray theory dictates that the leaky surface waves circumnavigate along the shell and then reradiate into the surrounding medium, out of which only the backwards energy can be received by the sensor. After the first reradiation, the subsequent ones will follow after each full circumnavigation. Therefore, the elastic waves appear as successive periodic sequences, a structure which might thus be exploited in order to improve the performance of the system.

In the following, we will exploit this structure, making use of a sparse recovery framework to estimate the time delays of the backscattered components. To address the periodic pattern of the elastic echoes, we model them as signal blocks, which may then be estimated exploiting a developed block sparse approach. Using this method, the weak components that may otherwise be ignored are incorporated in the signal structure using the inherent block structure of the signal, therefore improving the performance of the system.

II. Signal Model

For a spherical shell, and the broadside incidence of a cylindrical shell, the physical mechanism of the waves can be schematically represented as shown in Fig. 1. As illustrated, when an incident pulse propagates towards the shell, a specular reflection (in red) is produced, as well as leaky surface waves circumnavigating the shell (in green and yellow) and reradiating into the surroundings. The wave penetrates into the shell to excite surface waves with incidence angle of

This work was supported in part by the China Scholarship Council, the Swedish Research Council, the National Natural Science Foundation of China under Grant 11774073 and 51279033, and the Natural Science Foundation of Heilongjiang Province of China under Grant F201346.

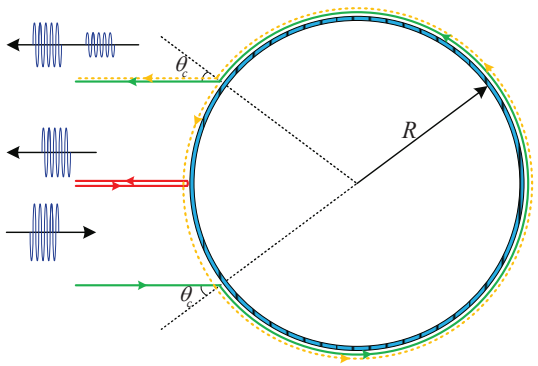

Fig. 1. Schematic diagram of the ray path scattering by a shell.

$\theta_c = \arcsin(c_w/c_g)$, where c_w is the speed of sound in water, and c_g the group velocity of the surface wave.

The received backscattered field can thus be approximated as the multiple replicas of the incidence signal. With $s_0(t)$ denoting the incidence waveform, the received signal can be expressed as

$$y(t) = \sum_{k=1}^{K} a_k s_0(t - \tau_k) + e(t) \tag{1}$$

where K denotes the number of signal components, a_k the amplitude of each components, which is assumed to be constant, and $e(t)$ an additive white Gaussian noise. The term $s_0(t - \tau_k)$ is a replica of $s_0(t)$ with a time-delay parameter τ_k.

With the assumption that a monostatic sonar system is located at a distance of L from the center of the shell, the travel time of the specular reflection is

$$\tau_s = \frac{2(L - R)}{c_w} \tag{2}$$

while for the first leaky surface wave the travel time is

$$\tau_{l,1} = \frac{2(L - R\cos\theta_c)}{c_w} + \frac{2(\pi - \theta_c)R}{c_g} \tag{3}$$

and for the following pth leaky surface wave

$$\begin{aligned}\tau_{l,p} &= \frac{2(L - R\cos\theta_c)}{c_w} + \frac{2(p\pi - \theta_c)R}{c_g} \\ &= \tau_{l,1} + (p-1)\Delta\tau_l \end{aligned} \tag{4}$$

where $\Delta\tau_l = 2\pi R/c_g$ is the time for a surface wave to circumnavigate along the shell for a whole circle. In this case, we can separate the signal term in (1) into two parts, which can be written as

$$\begin{aligned} y(t) &= a_s s_0(t - \tau_s) + \sum_{p=1}^{P} a_{l,p} s_0(t - \tau_{l,p}) + e(t) \\ &= a_s s_0(t - \tau_s) + \sum_{p=1}^{P} a_{l,p} s_0\big(t - \tau_{l,1} - (p-1)\Delta\tau_l\big) + e(t) \end{aligned} \tag{5}$$

Here, the leaky surface waves are considered as a group, i.e., a block pattern, which can be detailed by the parameters $\tau_{l,1}$, $\Delta\tau_l$, and p.

In the more general case, the signal model in (5) can be extended to have more components, such that

$$\begin{aligned} y(t) = &\sum_{n=1}^{N} a_n s_0(t - \tau_n) \\ &+ \sum_{m=1}^{M}\sum_{p=1}^{P_m} a_{m,p} s_0\big(t - \tau_{m,1} - (p-1)\Delta\tau_m\big) + e(t) \end{aligned} \tag{6}$$

where the first term represents the N individual waves resulting from specular reflections, and the second term consists of M blocks of elastic waves, in which there are P_m related periodic components,

Using a vector notation, the model in (1) can be expressed as

$$\mathbf{y} = \sum_{k=1}^{K} a_k \mathbf{s}_k + \mathbf{e} \tag{7}$$

which may be expressed using the block structure as

$$\mathbf{y} = \sum_{n=1}^{N} a_n \mathbf{s}_n + \sum_{m=1}^{M}\sum_{p=1}^{P_m} a_{m,p}\mathbf{s}_{m,p} + \mathbf{e} \tag{8}$$

where $\mathbf{y}$ and $\mathbf{e}$ are the received signal and noise terms, $\mathbf{s}_k$ represents the replica with time-delay τ_k, similarly for $\mathbf{s}_n$, while $\mathbf{s}_{m,p}$ is the pth part of the mth block with time-delay $(\tau_{m,1} + (p-1)\Delta\tau_m)$.

In (8), the first term can be regarded as being a special cases of the second term, although with only a single component being contained in each block. In this case, we can write (8) as

$$\mathbf{y} = \sum_{m=1}^{M}\sum_{p=1}^{P_m} a_{m,p}\mathbf{s}_{m,p} + \mathbf{e} \tag{9}$$

wherein not only the elastic parts, but also the individual parts are included.

With

$$\begin{aligned} \mathbf{A}_K &= \begin{bmatrix} a_1 & a_2 & \cdots & a_K \end{bmatrix}^T \\ \mathbf{S}_K &= \begin{bmatrix} \mathbf{s}_1 & \mathbf{s}_2 & \cdots & \mathbf{s}_K \end{bmatrix} \end{aligned}$$

the model in (7) can be expressed as

$$\mathbf{y} = \mathbf{S}_K \mathbf{A}_K + \mathbf{e} \tag{10}$$

Similarly, with

$$\begin{aligned} \mathbf{a}_m &= \begin{bmatrix} a_{m,1} & a_{m,2} & \cdots & a_{m,P_m} \end{bmatrix}^T \\ \mathbf{A}_M &= \begin{bmatrix} \mathbf{a}_1^T & \mathbf{a}_2^T & \cdots & \mathbf{a}_M^T \end{bmatrix}^T \\ \mathbf{s}_m &= \begin{bmatrix} \mathbf{s}_{m,1} & \mathbf{s}_{m,2} & \cdots & \mathbf{s}_{m,P_m} \end{bmatrix} \\ \mathbf{S}_M &= \begin{bmatrix} \mathbf{s}_1 & \mathbf{s}_2 & \cdots & \mathbf{s}_M \end{bmatrix} \end{aligned}$$

the model in (9) can be expressed as

$$\mathbf{y} = \mathbf{S}_M \mathbf{A}_M + \mathbf{e} \tag{11}$$

III. Time-delay estimation

Since there are only a few components (including specular reflection and elastic waves) that can be produced and received by the hydrophone, the estimation of the number of components and corresponding parameters can be obtained by a sparse reconstruction framework.

A. Lasso-based approach

For (10), since K is unknown, one may design a dictionary $\mathbf{W}$ containing many potential time-delayed replicas of the transmitted waveform, and then determine which component that can best represent the received signal. This is done by introducing the approximation

$$\mathbf{y} \approx \mathbf{W}\hat{\mathbf{A}}_w \tag{12}$$

where only the elements in coefficient vector $\hat{\mathbf{A}}_w$ that are relevant to these elements in $\mathbf{W}$ contained in the received signal are nonzero, while the others are zero. This representation allows the problem to be solved using the well-known Lasso estimator, such that [12], [13]

$$\underset{\mathbf{A}_w}{\text{minimize}} \frac{1}{2}\|\mathbf{y} - \mathbf{W}\mathbf{A}_w\|_2^2 + \lambda\|\mathbf{A}_w\|_1 \tag{13}$$

where the norm of the residual is used in the first term to enforce the reconstructed signal to be close to the received signal, as well as the ℓ_1-norm of the coefficient vector in the second term strives to make the solution sparse, that is to say, it forces the elements in $\mathbf{A}_w$ with small value to be zero. The relative importance of these two penalties is controlled by the tuning parameter λ. From the solution of this optimization problem, one may obtain the estimation of the number of components by counting the non-zero elements, and estimate the corresponding time delay using those in the dictionary. This form of optimization problem may be efficiently solved with using the Alternating Direction Method of Multipliers (ADMM) framework [14].

With a well-defined dictionary, this approach can achieve the parameters with high accuracy and resolution. However, one problem is that, if a component is relatively weak, there is a risk that it may be ignored. When applying this method to the backscattered echoes of a target, there is a risk that some parts, especially the weak elastic waves, may not be found or estimated.

B. Block sparse approach

We proceed to introduce a block sparse approach that avoids the risk of the Lasso-based method when the structure of the signal is periodic, as modeled in (11). Similar to the Lasso estimator, this method also needs to design a dictionary, here denoted $\mathbf{U}$. The difference is that $\mathbf{U}$ is defined with blocks of the periodic elements, which has a similar structure as $\mathbf{S}_M$ in (11), although with further structure. Reminiscent of the block sparse signal representation method used in multi-pitch estimation [15], the problem here can be solved using

$$\underset{\mathbf{A}_u}{\text{minimize}} \frac{1}{2}\|\mathbf{y} - \mathbf{U}\mathbf{A}_u\|_2^2 + \alpha\|\mathbf{A}_u\|_1 + \beta\sum_{d=1}^{D}\|\mathbf{a}_d\|_2 \tag{14}$$

where

$$\mathbf{A}_u = \begin{bmatrix}\mathbf{a}_1^T & \mathbf{a}_2^T & \cdots & \mathbf{a}_D^T\end{bmatrix}^T \tag{15}$$

is the overall coefficient vector consisting of the corresponding vector of each block. Herein, the first two terms are used to balance the residual and the sparsity of the solution. The third term is an added penalty, which can enhance the sparsity of the periodic patterns in the signal. Here, α and β are the tuning parameters which control the importance of these regularizations. By relaxing the ℓ_1-norm term, some components along with some noise or interference may be found. However, via the block term, only those ones with the expected pattern are kept, while others are removed. Thus, the optimization in (14) can not only reconstruct the sparse signal, but also find the weak components in patterns containing some strong reflections. By this approach, the structure of the signal can be used to decrease the probability of missing some components.

With the ADMM framework [14], the solution of (14) can be also obtained efficiently. By introducing the auxiliary variables $\mathbf{x}$ and $\mathbf{v}$, the problem in (14) may be equivalently expressed as

$$\begin{aligned}&\underset{\mathbf{x},\mathbf{v}}{\text{minimize}} \;\; f_1(\mathbf{x}) + f_2(\mathbf{v})\\ &\text{subject to} \;\; \mathbf{x} = \mathbf{v}\end{aligned} \tag{16}$$

where

$$f_1(\mathbf{x}) = \frac{1}{2}\|\mathbf{y} - \mathbf{U}\mathbf{x}\|_2^2 \tag{17}$$

$$f_2(\mathbf{v}) = \alpha\|\mathbf{v}\|_1 + \beta\sum_{d=1}^{D}\|\mathbf{v}_d\|_2 \tag{18}$$

with $\mathbf{x}$ and $\mathbf{v}$ having the same structure as $\mathbf{A}_u$. To solve the problem in (16), one may form the augmented Lagrangian

$$L_\rho(\mathbf{x}, \mathbf{v}, \mathbf{u}) = f_1(\mathbf{x}) + f_2(\mathbf{v}) + \frac{\rho}{2}\|\mathbf{x} - \mathbf{v} + \mathbf{u}\|_2^2 \tag{19}$$

wherein $\mathbf{u}$ is the introduced scaled dual variable. The ADMM solves the problem by iteratively minimizing the Lagrangian over each variable, resulting the $(i+1)$th steps as

$$\mathbf{x}^{(i+1)} = \underset{\mathbf{x}}{\text{argmin}} \;\; f_1(\mathbf{x}) + \frac{\rho}{2}\|\mathbf{x} - \mathbf{v}^{(i)} + \mathbf{u}^{(i)}\|_2^2 \tag{20}$$

$$\mathbf{v}^{(i+1)} = \underset{\mathbf{v}}{\text{argmin}} \;\; f_2(\mathbf{v}) + \frac{\rho}{2}\|\mathbf{x}^{(i+1)} - \mathbf{v} + \mathbf{u}^{(i)}\|_2^2 \tag{21}$$

$$\mathbf{u}^{(i+1)} = \mathbf{u}^{(i)} + \mathbf{x}^{(i+1)} - \mathbf{v}^{(i+1)} \tag{22}$$

The solution to (21) can be given by

$$\mathbf{x}^{(i+1)} = (\mathbf{U}^H\mathbf{U} + \rho\mathbf{I})^{-1}(\mathbf{U}^H\mathbf{y} + \rho(\mathbf{v}^{(i)} - \mathbf{u}^{(i)})) \tag{23}$$

while (22) can be solved by [15], [16]

$$\mathbf{v}^{(i+1)} = \overline{S}(S(\mathbf{u}^{(i)} + \mathbf{x}^{(i+1)}, \alpha/\rho), \beta/\rho) \tag{24}$$

where

$$\begin{aligned}S(\upsilon, \kappa)_i &= \frac{\upsilon_i}{|\upsilon_i|}\max(|\upsilon_i| - \kappa, 0)\\ \overline{S}(\upsilon, \kappa)_i &= \frac{\upsilon_i}{\|\upsilon_i\|_2}\max(\|\upsilon_i\|_2 - \kappa, 0)\end{aligned} \tag{25}$$

These steps are then repeated until convergence.

IV. Results

We proceed to examine the performance of the proposed block sparse estimator using both simulated and experimental signals.

A. Simulated signals

We begin by examining the synthetic backscattered echoes using a sequence of pulses corrupted by additive white Gaussian noise. The incidence pulse is a linear chirp signal formed as

$$s_0(t_n) = \exp(j2\pi f_0 t_n + j\pi k t_n^2) \tag{26}$$

where $k = (f_1 - f_0)/T_n$ is the frequency rate, with f_0 being the starting frequency, f_1 the ending frequency, and T_n the length of the signal. Herein, we set $f_0 = 0.03$ Hz, $f_1 = 0.08$ Hz, and $T_n = 1000$ samples. The simulated signal consists of 5 periodic replicas of the incidence pulse, in which the first has a 100 samples delay, and the interval between the following ones is 25 samples. The amplitudes of these replicas are set to be $a_1 = 0.8$, $a_2 = 0.4$, $a_3 = 0.2$, $a_4 = 0.1$, and $a_5 = 0.05$, respectively. The noise is added with a signal to noise ratio (SNR) of 0 dB, where the SNR is defined as

$$\text{SNR} = 10\log_{10}\frac{P_s}{\sigma^2} \tag{27}$$

wherein P_s represents the power of the signal and σ^2 is the variance of the noise.

The waveform of the signal is shown in Fig. 2, where the synthetic echoes are embedded in noise, which are clearly difficult to identify. We compare the results obtained by the Lasso-based approach and block sparse approach with the output of a matched filter, as shown in Figs. 3 and 4, respectively. The transmitted signal is used as the template of the matched filter. Because of the limited resolution of the matched filter, the estimation using the peaks of the output is biased. Besides, with the influence of the side-lobe of strong elements and the corruption of the additive noise, it can be seen that the 5th component cannot be estimated. In the results of the Lasso-based approach, the resolution and accuracy have been improved. As shown in Fig. 3, the first 3 components can be well estimated at the 100th, 125th, and 150th time points, while the latter 2 components cannot be determined. By adjusting the tuning parameter in (13), the weak components may be found, but some pseudo components may be introduced. As can be seen in Fig. 3, there are some false peaks around the true ones with amplitudes being even larger than the weak components. Using the block sparse approach, such problems can be avoided, as shown in Fig. 4. By exploiting the structure of the signal, all the 5 components can be well estimated. These results indicate that the block sparse method can achieve better performance for such periodic sequences as compared to the Lasso-based approach.

We proceed to examine the statistical performance of the proposed method using Monte Carlo simulations. At each noise level, 500 Monte Carlo simulations are used to obtain the presented results. As shown above, some of the components in the estimated results might be missing because their amplitudes are weak. To allow for this, we calculate the estimated rate of each component, which is counted only if the corresponding component is found and the estimated result is correct. The signal used is formed using the same frequency and amplitude parameters as before, using $T_n = 500$ samples. The first component in the signal is delayed uniformly over $[95, 105]$ samples, and the interval between the following ones is selected uniformly over $[21, 30]$ samples in each simulation. The rate of correct estimation of each component is shown in

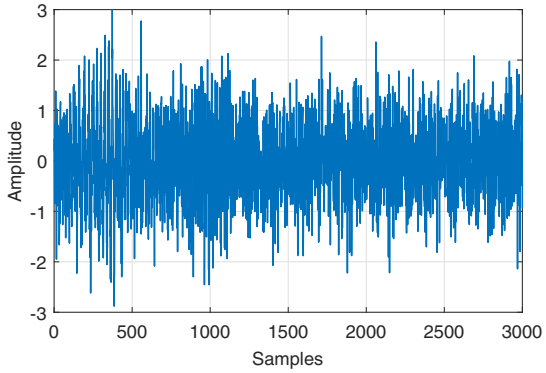

Fig. 2. The waveform of the simulated signal.

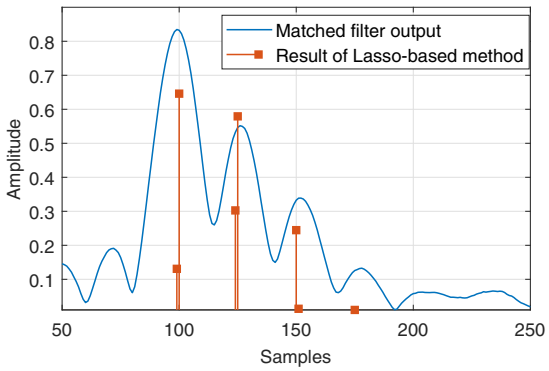

Fig. 3. The estimated results of Lasso-based approach.

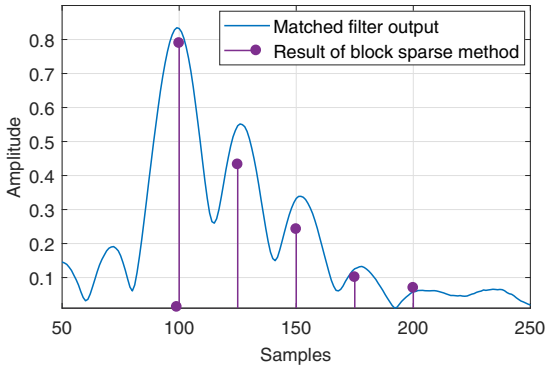

Fig. 4. The estimated results of block sparse approach.

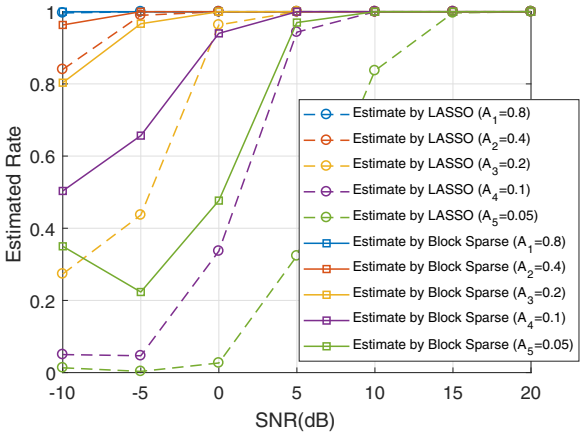

Fig. 5. The correct rate of estimating each component.

Fig. 5. It should be noted that the tuning parameters here vary at each noise level to ensure a proper setting with respect to the noise floor. From the results, it can be seen that the proposed block sparse method can consistently achieve a better result than the Lasso-based method. As seen in the figure, the block sparse approach can almost attain the same rate for a component as the Lasso-based method can do for the one that has twice the amplitude, suggesting that it can achieve the same performance as the Lasso-based approach, at an SNR level nearly 6dB lower than the Lasso-based method can.

B. Experimental results

An experiment was conducted in a tank to characterize the scattering field of a finite cylindrical shell with one hemispherical end-cap. The configuration of the experiment included a monostatic sonar system, a signal generation and acquisition system, and the shell along with a mechanical rotation system, as shown in Fig. 6. The tank was covered with anechoic wedges on all walls, bottom and water surface, making no other reflections, except for those reflected by the shell, being received. The sonar system transmitted a pulse, and measured the backscattered echoes. The shell was horizontally suspended by two strings, which were connected with a rotation system, driving the shell to rotate horizontally around its center. The sonar system and the shell were located at the same depth, with the distance between them being 6.78 m. The length of the shell was 2.10 m, including the hemispherical end-cap, the diameter was 0.53 m, and the thickness was 0.8 cm.

The pulse used in the experiment was a linear frequency modulated (LFM) signal, with instantaneous frequency sweeping from 10 kHz to 40 kHz over 0.5 ms. The corresponding reduced frequency kR ($k = \omega/c_w$ was the wavenumber in water) is 11 to 44, in which regime the enhancements due to the first antisymmetric Lamb wave (A_{0-}) can be observed [17]. With the rotation of the shell, the scattering field varying with incident angle can be obtained. The results with corresponding scattering structure are shown in Fig. 7,

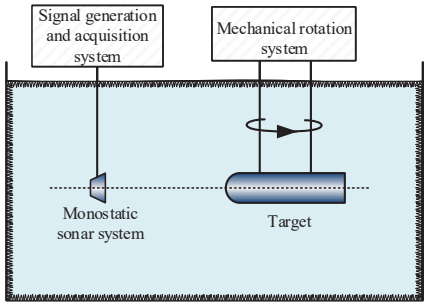

Fig. 6. The configuration of the tank experiment.

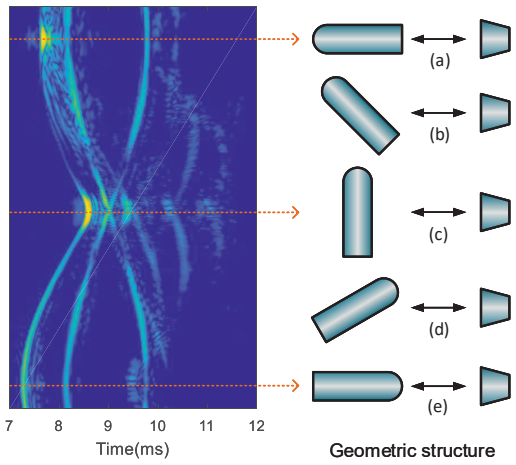

Fig. 7. The measured results varying with the relative position of the target and sonar system, mapped as the right part.

where each line represents a scattering component, including specular reflections by flat and hemispherical end-caps, the X-shaped pattern due to the scattering of the strings, and some elastic A_{0-} waves occurring after 10 ms. The special pattern we studied here is labeled as (c), where the incident direction is perpendicular to the axis of the shell, i.e., the broadside incidence. The corresponding echoes are displayed in Fig. 8, in which the waveform before 9.5 ms contains specular reflection and the scattering waves by the strings. The following clearly visible wave packets are the elastic A_{0-} waves. At this particular incidence, the influence of the hemispherical end-cap cannot be detected [18]. The main contribution is the cylindrical shell, for which the ray path can also be diagrammed as Fig. 1. Therefore, the travel time of each component can be predicted using (2) - (4). The value of the group velocity may be approximated as $1.33c_w$, i.e., 2000 m/s [6].

The proposed block sparse approach is used here to estimate the time delays of each components contained in Fig. 8. As comparisons, the results estimated by matched filter and the Lasso-based method are also presented. The transmitted pulse and time-delayed replica are used as the template of the matched filter and the elements in the dictionary, but the scattering components show different signatures. The main

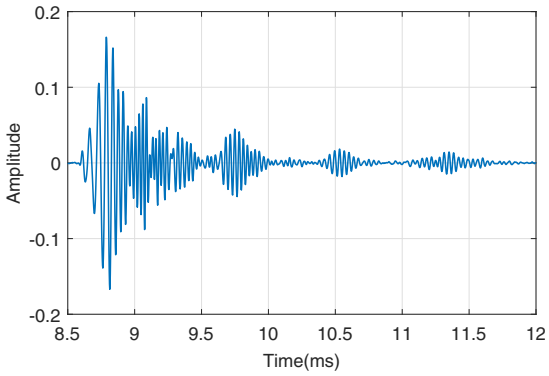

Fig. 8. The backscattered waveform measured on the broadside incidence.

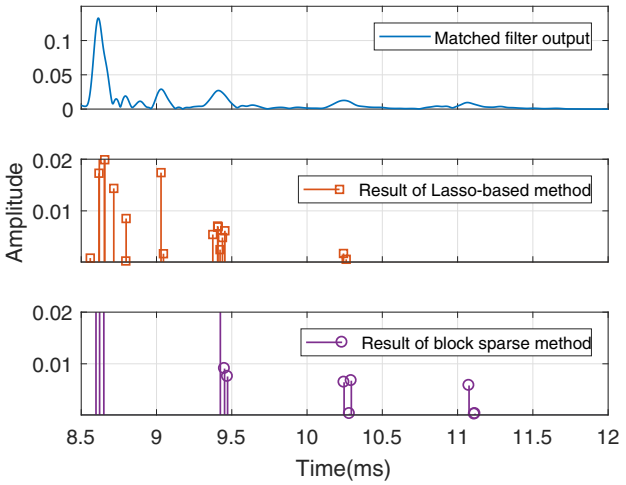

Fig. 9. The estimated results by matched filter, Lasso-based approach and the proposed block sparse approach.

TABLE I
THE ESTIMATED TRAVEL TIME.

	Specular reflection	Strings	1st A_{0-}	2ed A_{0-}	3rd A_{0-}
Theory	8.67	9.04	9.41	10.25	11.08
Matched filter	8.61	9.03	9.41	10.24	11.07
Lasso-based	8.62	9.03	9.41	10.24	–
Block sparse	8.62	–	9.42	10.25	11.08

lobes of the matched filter are quite wide, and the results by the sparse methods show groups corresponding to the scattering components. One should note that because of the use of the periodic pattern, the block sparse method can omit many more irrelevant components as compared to the Lasso-based results, while still retaining the components with weak power. The estimated travel time can be obtained by the extrema of each group, shown as Table I. The values show coincide with each other. Because the component due to the strings has no periodic pattern, and its power is weak, it is missed by the block sparse method.

V. Conclusion

By exploiting the inherent periodic structure of backscattered echoes of underwater shells, we introduce an estimator able to identify also weak reflectors, also using their contribution to improve on the estimation of the strong component. Further extension may be made to cases including, e.g., a reverberating background.

References

[1] J. A. Bucaro, B. H. Houston, M. Saniga, L. R. Dragonette, T. Yoder, S. Dey, L. Kraus, and L. Carin, "Broadband acoustic scattering measurements of underwater unexploded ordnance (UXO)," *J. Acoust. Soc. Am.*, vol. 123, no. 2, pp. 738–746, 2008.

[2] G. Kaduchak and P. L. Marston, "Observation of the midfrequency enhancement of tone bursts backscattered by a thin spherical shell in water near the coincidence frequency," *J. Acoust. Soc. Am.*, vol. 93, no. 1, pp. 224–230, 1993.

[3] G. Maze, "Acoustic scattering from submerged cylinders. MIIR Im/Re: Experimental and theoretical study," *J. Acoust. Soc. Am.*, vol. 89, no. 6, pp. 2559–2566, 1991.

[4] D. Décultot, R. Liétard, and G. Maze, "Classification of a cylindrical target buried in a thin sand-water mixture using acoustic spectra," *J. Acoust. Soc. Am.*, vol. 127, no. 3, pp. 1328–1334, 2010.

[5] A. M. Gunderson, A. L. España, and P. L. Marston, "Spectral analysis of bistatic scattering from underwater elastic cylinders and spheres," *J. Acoust. Soc. Am.*, vol. 142, no. 1, pp. 110–115, 2017.

[6] S. F. Morse and P. L. Marston, "Backscattering of transients by tilted truncated cylindrical shells: Time-frequency identification of ray contributions from measurements," *J. Acoust. Soc. Am.*, vol. 111, no. 3, pp. 1289–1294, 2002.

[7] S. D. Anderson, K. G. Sabra, M. E. Zakharia, and J.-P. Sessarego, "Time-frequency analysis of the bistatic acoustic scattering from a spherical elastic shell," *J. Acoust. Soc. Am.*, vol. 131, no. 1, pp. 164–173, 2012.

[8] F. J. Blonigen and P. L. Marston, "Leaky helical flexural wave backscattering contributions from tilted cylindrical shells in water: Observations and modeling," *J. Acoust. Soc. Am.*, vol. 112, no. 2, pp. 528–536, 2002.

[9] Z. Xia, X. Li, and X. Meng, "High resolution time-delay estimation of underwater target geometric scattering," *Elsevier Appl. Acoust.*, vol. 114, pp. 111–117, 2016.

[10] H. Jia, X. Li, and X. Meng, "Rigid and elastic acoustic scattering signal separation for underwater target," *J. Acoust. Soc. Am.*, vol. 142, no. 2, pp. 653–665, 2017.

[11] K. G. Sabra and S. D. Anderson, "Subspace array processing using spatial time-frequency distributions: Applications for denoising structural echoes of elastic targets," *J. Acoust. Soc. Am.*, vol. 135, no. 5, pp. 2821–2835, 2014.

[12] H. He, T. Yang, and J. Chen, "On time delay estimation from a sparse linear prediction perspective," *J. Acoust. Soc. Am.*, vol. 137, no. 2, pp. 1044–1047, 2015.

[13] Y. Park, W. Seong, and Y. Choo, "Compressive time delay estimation off the grid," *J. Acoust. Soc. Am.*, vol. 141, no. 6, pp. EL585–EL591, 2017.

[14] S. Boyd, N. Parikh, E. Chu, B. Peleato, and J. Eckstein, "Distributed optimization and statistical learning via the alternating direction method of multipliers," *Found. Trends Mach. Learn.*, vol. 3, no. 1, pp. 1–122, 2011.

[15] S. I. Adalbjörnsson, A. Jakobsson, and M. G. Christensen, "Multi-pitch estimation exploiting block sparsity," *Elsevier Sign. Process.*, vol. 109, pp. 236 – 247, 2015.

[16] R. Chartrand and B. Wohlberg, "A nonconvex ADMM algorithm for group sparsity with sparse groups," in *2013 IEEE International Conference on Acoustics, Speech and Signal Processing*, May 2013, pp. 6009–6013.

[17] S. F. Morse, P. L. Marston, and G. Kaduchak, "High-frequency backscattering enhancements by thick finite cylindrical shells in water at oblique incidence: Experiments, interpretation, and calculations," *J. Acoust. Soc. Am.*, vol. 103, no. 2, pp. 785–794, 1998.

[18] N. Touraine, L. Haumesser, D. Décultot, G. Maze, A. Klauson, and J. Metsaveer, "Analysis of the acoustic scattering at variable incidences from an extra thin cylindrical shell bounded by hemispherical endcaps," *J. Acoust. Soc. Am.*, vol. 108, no. 5, pp. 2187–2196, 2000.